Heteroatom Chemistry
Volume 12, Number 5, 2001

# π-Facial Diastereoselection of Hydride Reduction of 1,3-diheteran-5-ones: Application of the Exterior Frontier Orbital Extension Model

Daisuke Kaneno, Jian Zhang, Michio Iwaoka, and Shuji Tomoda

*Department of Life Sciences, Graduate School of Arts and Sciences, The University of Tokyo, Komaba, Meguro-Ku, Tokyo 153-8902, Japan*

*Received 4 January 2001; revised 21 February 2001*

ABSTRACT: *To obtain further evidence for the importance of the ground state conformational and orbital properties in π-facial diastereoselection of 1,3-diheteran-5-ones (heteroatom = O, S, Se), 2-phenyl-1,3-diselenan-5-one (***3a***) has been synthesized, and its π-facial diastereoselection upon hydride reduction has been examined. The experimental data of π-facial stereoselection of* **3a** *has been successfully rationalized by the exterior frontier orbital extension model (the EFOE model). Intrinsic reaction coordinate (IRC) and natural bond orbital (NBO) analyses of transition states of $LiAlH_4$ reduction of this ketone have strongly indicated that the transition state effects (the torsional strain of the carbonyl moieties and the antiperiplanar effects involving the incipient bond proposed by the conventional theoretical models for π-facial diastereoselection; the Felkin-Anh model and the Cieplak model) are not responsible for facial selection.* © 2001 John Wiley & Sons, Inc. Heteroatom Chem 12:358–368, 2001

## *INTRODUCTION*

The origin of π-facial diastereoselection in nucleophilic addition reactions to carbonyl substrates has been the subject of intense debate for half a century [1]. Diastereoselectivity has been rationalized by various stabilization mechanisms, especially in terms of the antiperiplanar hyperconjugative effect (hereafter abbreviated as the *AP effect*) that emphasizes the importance of the interaction between the incipient bond and an adjacent AP bond in the transition state (the Felkin-Anh model [2] and the Cieplak model [3]). As a consequence, most arguments are based on the transition state stabilization effects. However they have been discussed without quantitative evaluation. Recently we have proposed a new theoretical model (the exterior frontier orbital extension model [EFOE]) to explain and predict the π-facial diastereoselection of nucleophilic addition to carbonyl compounds [4]. This model is based on the simple assumption that the facial difference in the reaction driving force between the two carbonyl faces must be the origin of π-facial diastereoselection [5]. Two quantities corresponding to the first term (exchange repulsions and steric effect) and the third term (donor–acceptor stabilizing interactions) of the Salem-Klopman equation [6], namely π-plane-divided exterior frontier orbital electron density (EFOE density) and π-plane-divided accessible space (PDAS), were defined (See appendix). Remarkable predictive power of this simple semiquantitative model has been shown using a variety of cyclic ketone substrates including substituted cyclohexanones, decalones, adamantanones, bicyclic ketones, 4-piperidones, imines, and iminium ions [7]. Very

*Correspondence to:* Shuji Tomoda.

recently we have reported another successful application of the EFOE model to 1,3-diheteran-5-ones (heteroatom = O, S; **1** and **2**) [8].

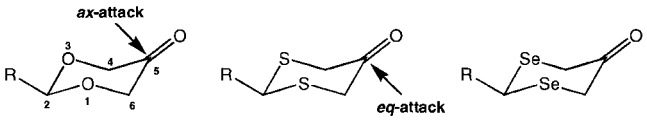


The unique reversal of face selection in nucleophilic additions of 2-phenyl-1,3-dioxan-5-one (**1a**) and 2-phenyl-1,3-dithian-5-one (**2a**) has been a controversial debate since the early 1980s [3]. $LiAlH_4$ reduction and the Grignard reaction of **1a** gave the equatorial alcohol predominantly via axial attack (92–97%) [9] even when bulky reagents, such as iso-PrMgI or *tert*-BuMgI, were employed. Jochims interpreted these results in terms of reduced steric hindrance in the axial face of **1a** owing to the lack of two axial hydrogens at the 1- and 3-positions in the 6-membered ring. Interestingly, their subsequent studies using the sulfur analog (**2a**) indicated complete stereochemical reversal in nucleophilic additions of **2a** with $LiAlH_4$ and Grignard reagents (85–93%) [10].

Wu and Houk performed MM2 force field calculations of the parent compounds (**1b** and **2b**) and proposed the torsional strain to be responsible for the observed stereochemistry [11]. On the other hand, Cieplak interpreted these results according to his assumption of the order in the electron-donating abilities of the antiperiplanar bonds (C–S > H–H > C–C > C–O) [3]. Wu and Houk disclosed criticism against Cieplak's hypothesis to propose again the torsional strain model with strong emphasis on the electrostatic solvent interaction with heteroatoms [12].

Herein we describe further successful application of the EFOE model [13] to the hydride reduction of the selenium analog of 1,3-diheteran-5-ones (**3**).

## *COMPUTATIONAL METHODS*

Ab initio molecular orbital calculations were performed with GAUSSIAN 94 and GAUSSIAN 98 [14]. The Becke three-parameter hybrid functional combined with the Lee, Yang, and Parr (LYP) correlation functional, denoted as B3LYP [15], or with the nonlocal correlation provided by the Perdew 91 expression (B3PW91) [16], was employed in the calculations using the density functional theory (DFT). Geometries of transition states were optimized with the Huzinaga basis set [17] for Se and 6–31G(d) basis set for other atoms. Vibrational analyses were performed for all transition states to confirm that they have only one imaginary frequency. Intrinsic reaction coordinate (IRC) and natural bond orbital (NBO) [18] analysis were carried out at the HF/3-21G(d) level. HF level geometry optimizations were used for all substrates with the Huzinaga basis set for Se and 6-31G(d) basis set for other atoms. The EFOE model analyses were performed using our program [19].

## *RESULTS AND DISCUSSION*

### *Synthesis and Reduction of* **3a**

Synthesis of the model compound (2-phenyl-1,3-diselenan-5-one; **3a**) is shown in Scheme 1. Treatment of 2,3-dichloro-1-propene with *N*-bromosuccinimide (NBS) in methanol gave 1-bromo-3-chloro-2,2-dimethoxypropane in 84% yield. Acidic acetal exchange of the dimethoxyacetal with ethylene glycol followed by reaction with $Na_2Se_2$ gave the ethylene glycol acetal of 3,4-diselenacyclopentan-1-one (**4**) in 33% yield [20]. Compound **4** was allowed to react with $NaBH_4$ in the presence of dibromophenylmethane to give the acetal of the desired compound (**5**), which was hydrolyzed with TsOH to obtain the desired model compound (**3a**) in 76% overall yield from **4**.

Reduction of **3a** with $LiAlH_4$ ($Et_2O$, room temperature [r.t.]) quantitatively provided a 10:90 mixture of the equatorial and axial alcohols (**6a** and **6b**). Similarly, $NaBH_4$ (MeOH, r.t.) reduction afforded a 6:94 mixture of **6a** and **6b** in 98% yield. In either case, equatorial hydride delivery was preferred. The ratio was obtained by integration of the benzyl hydrogen signal (5.33, 5.23 ppm for the equatorial alcohol and the axial alcohol, respectively) of their $^1H$ NMR spectra. The stereochemistry of the major product (**6b**) was confirmed by X-ray crystallo-

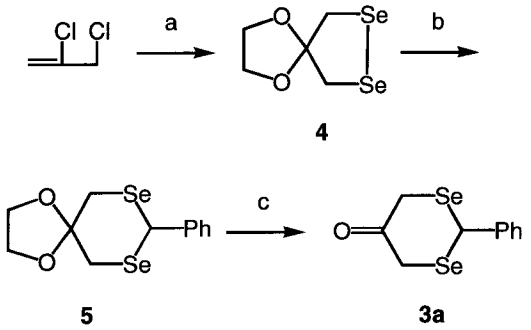


a: NBS; $CH_2(OH)CH_2OH$; $Na_2Se_2$. b: $NaBH_4$, $PhCHBr_2$. c: TsOH.

**SCHEME 1**

graphic analysis, which indicated that the phenyl and the hydroxyl groups are on the equatorial and the axial orientation, respectively (Figure 1). Therefore, it is concluded that the metal hydride reduction of 2-phenyl-1,3-diselenan-5-one (**3a**) gave similar results as those of 2-phenyl-1,3-dithian-5-one (**2a**): the axial alcohol generated by equatorial attack is the major product.

## *TRANSITION STATE ANALYSIS*

### *Structures*

The transition state (TS) structures for the reduction of **3b** with $LiAlH_4$ are shown in Figure 2 and summarized in Table 1 along with those of other systems for comparison. Like other 1,3-diheteran-5-ones systems, the imaginary frequency of the equatorial transition state (eq-TS) for **3b** ($\nu_i = -201.1$ cm$^{-1}$) is greater than the corresponding value of the axial transition state (ax-TS) ($\nu_i = -146.6$ cm$^{-1}$). Each vibrational mode corresponds to the stretching vibration of the incipient bond. The structures around the reaction center are similar to those of the other 1,3-diheteran-5-ones [21]. Comparison between the transition state data of the 1,3-diheteran-5-ones (**1b, 2b**, and **3b**) reveals that (1) the hydride approaching angles ($\theta$) and the torsional angles between the incipient bond and the vicinal antiperiplanar bond (the AP bond) ($\phi$) are nearly the same, but (2) as chalcogen atoms becomes heavier, the incipient bond distances ($C_{=O}\cdots H$) of the ax-TS get longer (1.862, 1.952, and 2.090 Å for X = O, S, Se, respectively), whereas the corresponding values of the eq-TS get shorter (1.716, 1.544, and 1.451 Å, respectively).

Table 2 presents the data of vibrational analysis for **3b** along with those of **1b** and **2b**. Relative total electronic energy (ZPVE-corrected) between the axial transition state (ax-TS) and the equatorial one (eq-TS) for **3b** is $-3.68$ kcal mol$^{-1}$ in favor of the eq-TS. Corresponding values of **1b** and **2b** are 2.65 and $-1.61$ kcal mol$^{-1}$, respectively, in agreement with the experimental stereoselectivity.

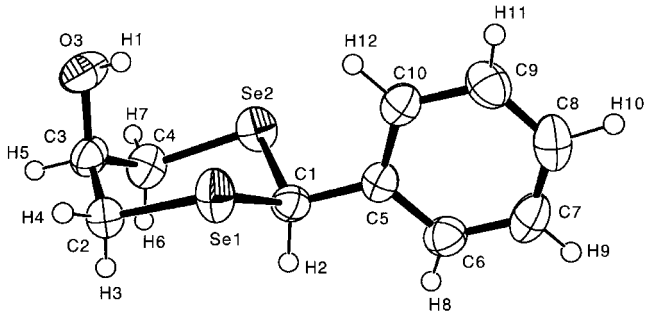


**FIGURE 1** Molecular structure of **6b** in the crystal.

## *TRANSITION STATE STABILIZATION EFFECTS*

Recently, we reported that the results of the theoretical transition state analysis were inconsistent with the conventional transition state models [4]. It should be noted that the new data of transition state analysis for **3b** are in accord with the previous conclusion that the AP effects operate against facial diastereoselection. Table 3 shows the quantitative evaluation of the antiperiplanar hyperconjugative stabilization effect (the AP effect) obtained by computing the magnitude of the antiperiplanar bond elongation as well as by natural bond orbital (NBO) analysis [18]. The $LiAlH_4$ transition states of **3b** (X = Se) show significant difference in percent bond elongation (%BE) [22] of the antiperiplanar bonds vicinal to the incipient bond ($C4–H4_{ax}$/$C6–H6_{ax}$ for ax-TS or C4-Se3/C6-Se1 for eq-TS) due to the AP effect between the ax-TS (+0.38%) and the eq-TS (−0.31%) relative to the ground-state **3b** optimized at the same level. The relative magnitude of these AP effects is clearly inconsistent with the observed facial selection for **3a**. It is surprising that the %BE value for the eq-TS is negative, suggesting bond (C–Se) shortening rather than elongation at the transition state. In consonant with these results, the difference in NBO bond population (ΔBP), obtained at the same level and method as employed for transition structure calculations, for the antiperiplanar bonds between the transition state and the ground state was $-0.0244$ e (electrons) for ax-TS and $-0.0077$ e for eq-TS. The greater ΔBP for the former is again consistent with the greater AP effect in ax-TS. Hence, the AP effects are apparently operating against the observed stereoselectivity for **3b** as observed previously for the reduction of cyclohexanone, adamantanone, **1b** and **2b** [7,21]. We emphasize here once again that the AP effect should be regarded as an internal energy relaxation mechanism that operates against the direction of bond formation process [4].

## *INTRINSIC REACTION COORDINATE (IRC) ANALYSIS*

Intrinsic reaction coordinate (IRC) analysis provided further evidence for the remarkable conclusions drawn from the previous transition state analyses. Figure 3 depicts (a) plots of bond elongation of the antiperiplanar bonds (%BE) against the IRC and (b) plots of the amount of reduced bond population of the antiperiplanar bonds relative to the electron

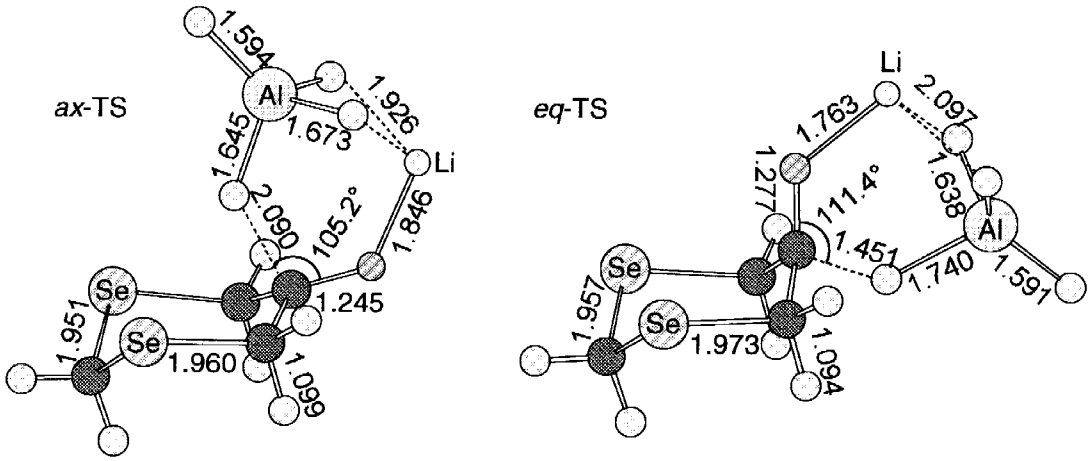


**FIGURE 2** Transition state structures of $LiAlH_4$ reduction of 1,3-diselenan-5-one (**3b**) (B3PW91/Huzinaga basis for Se and 6-31G(d) for C, H, O, Al and Li).

**TABLE 1** Selected Structural Parameters for the Transition States (TS) of 1,3-Diheteran-5-ones (**1b, 2b** and **3b**; X = O, S, Se) and Cyclohexanone Reduction with $LiALH_4$[a,b]

| *Compounds* | *TS* | $\nu_i^c$ | $\theta^d$ | $C_{=O}\cdots H^e$ | $\phi^f$ | $H-Al$ | $O\cdots Li$ | $C{=}O$ | $C_{=O}-C_\alpha$ | $C_\alpha - X_\beta$ |
|---|---|---|---|---|---|---|---|---|---|---|
| **1b** | ax | −290.7 | 108.6 | 1.862 | 177.2 | 1.660 | 1.822 | 1.254 | 1.525 | 1.419 |
| | eq | −340.3 | 109.0 | 1.716 | 152.1 | 1.688 | 1.796 | 1.258 | 1.536 | 1.434 |
| **2b** | ax | −234.6 | 106.4 | 1.952 | 177.3 | 1.652 | 1.830 | 1.252 | 1.524 | 1.829 |
| | eq | −383.3 | 110.0 | 1.544 | 167.2 | 1.720 | 1.770 | 1.243 | 1.535 | 1.842 |
| **3b** | ax | −146.6 | 105.2 | 2.090 | 173.3 | 1.645 | 1.846 | 1.245 | 1.512 | 1.960 |
| | eq | −201.1 | 111.4 | 1.451 | 171.0 | 1.740 | 1.763 | 1.277 | 1.529 | 1.973 |
| Cyclohexanone | ax | −377.7 | 109.8 | 1.531 | 177.6 | 1.709 | 1.764 | 1.284 | 1.531 | 1.536 |
| | eq | −392.6 | 109.5 | 1.556 | 161.6 | 1.702 | 1.771 | 1.283 | 0.153 | 1.547 |

[a]Calculated at the B3LYP/6-31+G(d) level (X = O, S), B3PW91/6-31G(d) with Huzinaga basis for Se.
[b]Angles in degree and bond distances in Å.
[c]Imaginary vibrational frequency ($cm^{-1}$).
[d]The angle between the incipient bond and the carbonyl bond.
[e]Distance of the incipient bond.
[f]The torsion angle between the incipient bond and the vicinal antiperiplanar bond.

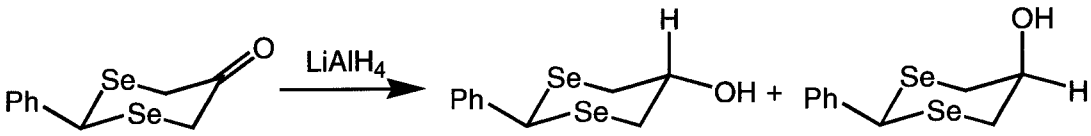


**3a** **6a** **6b**

**SCHEME 2**

population of the corresponding bond of substrate ketone (ΔBP) against the IRC. In both axial and equatorial processes, the AP effects (roughly) monotonically decrease toward transition states. Moreover, these results indicate that they operate against observed facial stereoselection. In the reduction of **3b**, the AP effects in the process toward eq-TS are always smaller than those in the corresponding axial process. In particular, the preferred equatorial process of the reaction of **3b** shows negative %BE all the way along the IRC, indicating that the antiperiplanar bonds become shorter than those in the initial substrate ketone throughout this process. Similar trends were observed in 1,3-dithian-5-one systems [21]. All

**TABLE 2** Vibrational Analysis of the Transition States (TS) of 1,3-diheteran-5-ones (**1b, 2b**, and **3b**; X = O, S, Se) and Cyclohexanone Reduction with $LiALH_4$[a]

| *Compounds* | *TS* | *Freq.*[b] | *ZPVE*[c] | *E*[d] | *ΔE*[e] |
|---|---|---|---|---|---|
| **1b** | ax | −290.7 | 83.75 | −634.07726 | 2.65 |
| | eq | −340.3 | 83.96 | −634.07336 | |
| **2b** | ax | −234.6 | 78.97 | −1280.02383 | −1.61 |
| | eq | −383.3 | 79.42 | −1280.02712 | |
| **3b** | ax | −146.6 | 77.44 | −5282.42236 | −3.68 |
| | eq | −201.1 | 77.96 | −5282.42905 | |
| Cyclohexanone | ax | −377.7 | 113.97 | −562.29163 | 1.36 |
| | eq | −392.6 | 114.12 | −562.28970 | |

[a]Calculated at the B3LYP/6-31+G(d) level (X = O, S), B3PW91/6-31G(d) with Huzinaga basis for Se.
[b]Imaginary vibrational frequency ($cm^{-1}$).
[c]Zero point vibrational energy in kcal $mol^{-1}$.
[d]Total electronic energy in au.
[e]ZPVE-corrected energy difference in kcal $mol^{-1}$.

**TABLE 3** Selected Parameters for the Transition States (TS) Structures and Antiperiplanar Effects of 1,3-Diheteran-5-ones (**1b, 2b**, and **3b**; X = O, S, Se) Reduction with $LiALH_4$[a,b]

| | | | | *C4-$H_{ax}$ (C6-$H_{ax}$)* | | *C4-X3 (C6-X1)* | |
|---|---|---|---|---|---|---|---|
| *X* | *TS* | *ϕ*[c] | *τ*[d] | *(Å) (%BE)*[f] | *BP*[e] *(ΔBP)*[g] | *(Å) (%BE)*[f] | *BP*[e] *(ΔBP)*[g] |
| O | ax | 177.2 | 32.0 | 1.106 (+0.11%) | 1.9606 (−0.0068) | | |
| | eq | 152.1 | 55.2 | | | 1.434 (+0.62%) | 1.9806 (−0.0081) |
| S | ax | 177.3 | 42.3 | 1.101 (+0.25%) | 1.9584 (−0.0188) | | |
| | eq | 167.2 | 70.3 | | | 1.842 (−0.11%) | 1.9679 (−0.0002) |
| Se | ax | 173.3 | 44.5 | 1.0987 (+0.38%) | 1.95642 (−0.0244) | | |
| | eq | 171.0 | 74.0 | | | 1.9703 (−0.31%) | 1.96323 (−0.0077) |

[a]Calculated at the B3LYP/6-31+G(d) level (X = O, S), B3PW91/6-31G(d) with Huzinaga basis for Se.
[b]Angles in degree and bond distances in Å.
[c]The torsion angle between the incipient bond and the vicinal antiperiplanar bond.
[d]Dihedral angle between C4–C5 and C6–X1 bond.
[e]Bond population calculated with NBO analysis.
[f]Percent bond elongation (+) or shrinkage (−) relative to the corresponding bond distance of ground-state 1,3-diheteran-5-one optimized at the B3LYP/6-31 + G(d) level.
[g]Difference on bond population of the corresponding bond between TS and ground-state 1,3-diheteran-5-one optimized at the B3LYP/6-31 + G(d) level.

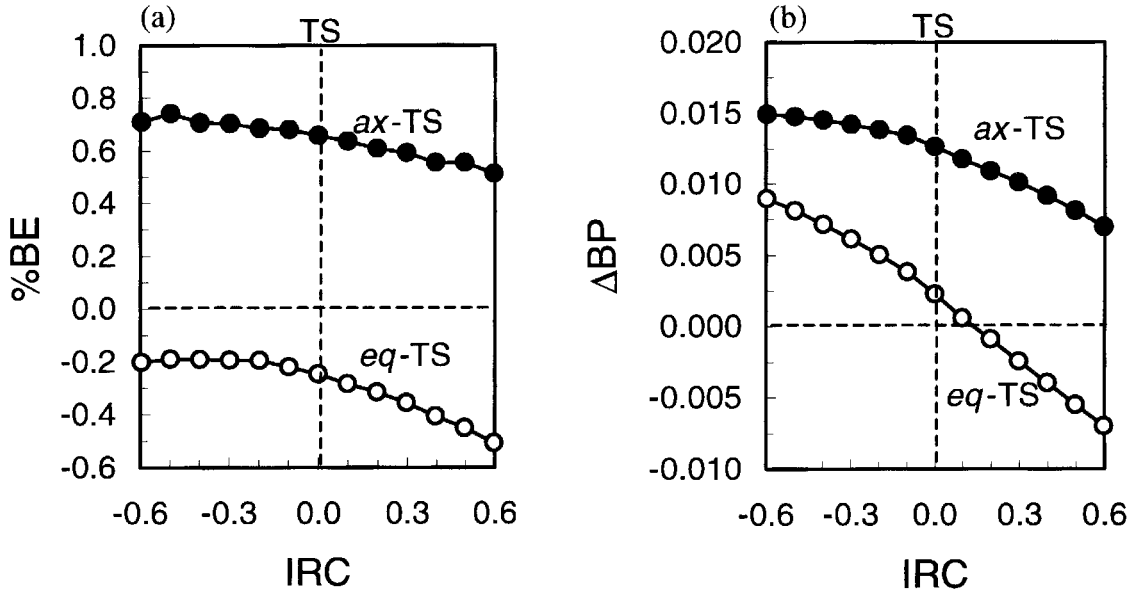


**FIGURE 3** Plot of (a) % elongation of the antiperiplanar bonds (%BE) and (b) reduced bond population for the antiperiplanar bonds (ΔBP) against IRC (unit; amu$^{1/2}$ bohr) for the $LiAlH_4$ reduction of **3a** (HF/3-21G(d) using Huzinaga basis for Se).

these theoretical observations strongly suggest the following two remarkable statements: (1) the AP effects operate effectively in the initial process and they are attenuated steadily toward the transition state and (2) they operate against observed facial diastereoselection.

In agreement with these conclusions, NBO analysis along the IRC toward transition states suggested that the amount of reduced bond population of the antiperiplanar bonds relative to the electron population of the corresponding bond of substrate ketone (ΔBP) monotonically decrease along the IRC as shown in Figure 3b. This again clearly suggests that the strength of the antiperiplanar bonds increases toward the transition state and is entirely consistent with the trends exhibited by %BE (Figure 3a).

## *APPLICATION OF THE EFOE MODEL*

The significant conclusion drawn from the previous discussion is that transition state effects may not be an essential factor of diastereoselection in these nucleophilic carbonyl additions. Considering these results as well as the origin of $\pi$-facial diastereoselection again, the element of diastereoselection would be the $\pi$-facial difference in rate constants rather than transition state events. Accordingly, we have applied here again the exterior frontier orbital extension model (the EFOE Model) [4]. This model assumes that the ground state conformational and the electronic properties may be responsible for the observed stereoselection of **3a**. The results of EFOE analysis using $\pi^*_{C=O}$ orbital (lowest unoccupied molecular orbital [LUMO] + 2 for **3a** and LUMO for **3b**), collected in Table 4 along with those of **1** and **2** for comparison, are entirely consistent with experimental diastereoselectivity. Enhanced preference for equatorial hydride ($LiAlH_4$) attack at **3a** (ax:eq = 10:90) compared with 2a (ax:eq = 15:85) is consistent not only with the marginal axial values of EFOE density (0.043% for **3a** and 0.299% for **2a**) but also with PDAS values (10.5 atomic unit (au)$^3$ for **3a** and 17.9 au$^3$ for **2a**). Moreover, the $\pi$-facial differences in the PDAS values between **1a** and **2a** clearly indicating that the steric environment around their carbonyl carbons is opposite with each other. Hence the facial diastereoselection for **3a** is both orbital- and

**TABLE 4** EFOE Analysis of **1, 2, 3**, and Cyclohexanone and Observed Diastereoselectivity (ax:eq)[a]

| | *EFOE Density (%)*[b] | | *PDAS (au$^3$)*[c] | | *Obs. (%)* |
|---|---|---|---|---|---|
| *Compd.* | *ax* | *eq* | *ax* | *eq* | *ax:eq* |
| Cyclohexanone | 1.940 | 0.249 | 19.4 | 47.2 | 92:8 |
| **1a** | 1.279 | 0.245 | 67.6 | 26.5 | 94:6 |
| **1b** | 1.739 | 0.243 | 71.2 | 26.2 | — |
| **2a** | 0.299 | 0.882 | 17.9 | 55.4 | 15:85 |
| **2b** | 0.277 | 0.834 | 18.4 | 54.6 | – |
| **3a** | 0.056 | 0.764 | 10.4 | 62.9 | 10:90 |
| **3b** | 0.043 | 0.682 | 10.5 | 62.4 | — |

[a]Calculated at the HF/6-31G(d) level using Huzinaga basis for Se.
[b]$\pi$-Plane-divided exterior frontier orbital electron density.
[c]$\pi$-Plane-divided accessible space.

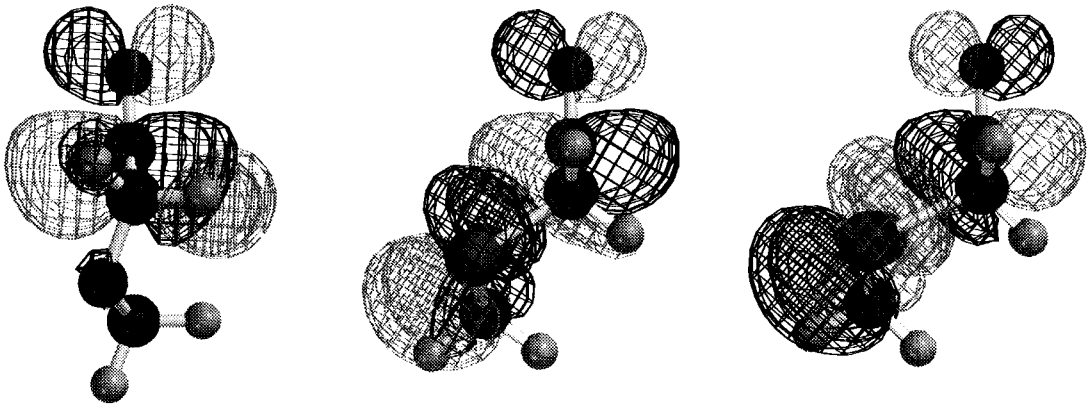


**FIGURE 4** Side views of the LUMOs of **1b, 2b**, and **3b** (HF/6-31G(d)).

steric-controlled like other 1,3-diheteran-5-ones (**1a, 2a**) [21] in sharp contrast to cyclohexanone, which is orbital controlled [13].

Figure 4 depicts the side views of the conformations and LUMOs of **1b, 2b**, and **3b** optimized at the HF/6-31G(d) level. It is interesting to note that the conformation of **3b** around the carbonyl is more puckered than that of **2b** (torsion angle along O=C5–C6–Se1; $\tau$ = 107.4°, O=C5–C6–S1; $\tau$ = 115.9°, respectively). The puckering of **3a** causes an increase in PDAS values at the equatorial face. On the other hand, the geometry of **1b** around the carbonyl is nearly planar (torsion angle along O=C5–C6–O1; $\tau$ = 158.5°), which leads to the enormous steric relaxation at the axial face.

Thus the facial diastereoselection of these substrate ketones can be reasonably explained by their ground state frontier orbital extension (EFOE density) and conformation (PDAS).

## *CONCLUSIONS*

### *Origin of Conformational Deformation*

The results disclosed in the previous sections suggest that the origin of facial diastereoselection may be attributed to the uniqueness of the ground state properties of **3** rather than to the transition state antiperiplanar effects involving the incipient bonds. Figure 5 shows the side views of optimized **1b, 2b**, and **3b** along with 1,3-ditelluran-5-one. It is immediately recognized that their six-membered rings are more folded on going from left to right (O to Te). The $\phi$ values (the angle between the carbonyl plane and the plane containing X1, X3, C4, and C6) steadily increase on going from light to heavier chalcogenides (156.6°, 123.1°, 116.4°, 110.4° for O, S, Se, Te, respectively). In consonance with such a trend, the PDAS values over the axial face of the carbonyl plane steadily decrease (71.2, 18.4, 10.4, and 6.3 au$^3$ for O, S, Se, Te, respectively). The mechanism of conformational deformation of six-membered rings containing heteroatom(s) is commonly ascribed to changes in bond angles and lengths owing to the unique covalent properties of heteroatoms [23]. However, in the presence of a functional group possessing low-lying local LUMOs such as carbonyl, another factor that affects significantly the conformation of the system may become important, since electron delocalization that occurs via vacant local molecular orbital(s) (MO) [24] is greatly facilitated by the presence of both low-lying unoccupied local MO(s) and nearby high-lying occupied MO(s). Since the order of the latter for the four heterocycles depicted in Figure 5 is $\sigma_{CTe} > \sigma_{CSe} > \sigma_{CS} > \sigma_{CO} >$, it is expected that the hyperconjugative stabilization between these orbitals and carbonyl orbital may play an important role on molecular conformation.

Table 5 shows the results of NBO analysis of four analogs of 1,3-diheteran-5-ones (heteroatom = O, S, Se, Te). It is shown that hyperconjugative electron delocalization around the carbonyl $\pi$ bond is significant. Cieplak mode indicates the hyperconjugation from antiperiplanar bonds to carbonyl carbon, while Felkin-Anh mode indicates the other way (from carbonyl carbon to antiperiplanar bonds). Each of them is further classified into two mechanisms. It is clearly revealed that **1b** (X = O) prefers the hyperconjugation between $\sigma_{C4H4ax}$ and $\pi_{C=O}$. On the other hand, heavy chalcogenides (X = S, Se, Te) prefer the hyperconjugation between $\sigma_{X3C4}$ and $\pi_{C=O}$.

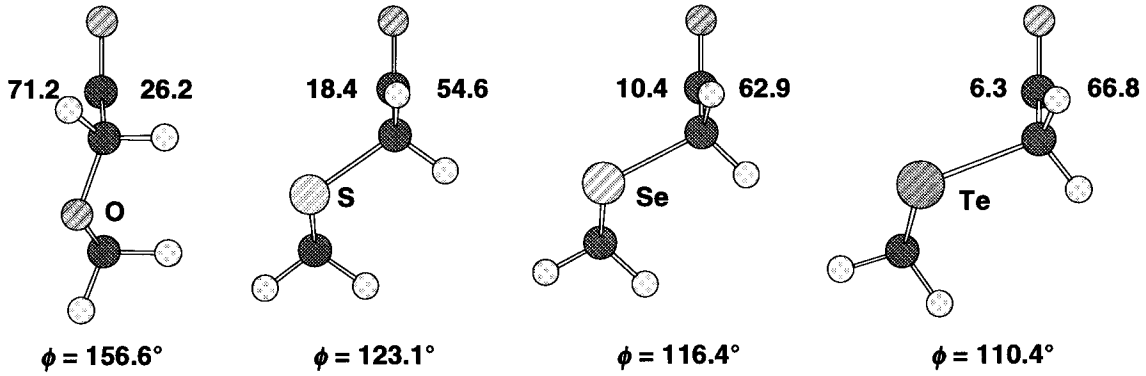


**FIGURE 5** Side views of 1,3-diheteran-5-ones (heteroatom = O, S, Se, Te) (HF/6-31G(d)). $\phi$ denotes the folding angle between the carbonyl plane and the X1-X3-C4-C6 plane. Numerical values indicated in the structures are PDAS in au[3].

**TABLE 5** Antiperiplanar Hyperconjugation Involving the $\pi_{C=O}$ Orbital in 1,3-Diheteran-5-ones (Heteroatom = O, S, Se Te) (kcal mol$^{-1}$)[a]

| | *Cieplak Mode* | | *Felkin-Anh Mode* | |
|---|---|---|---|---|
| *Heteroatom* | $\sigma_{C4H4ax} \rightarrow \pi^*_{C=O}$ | $\sigma_{X3C4} \rightarrow \pi^*_{C=O}$ | $\pi_{C=O} \rightarrow \sigma^*_{C4H4ax}$ | $\pi_{C=O} \rightarrow \sigma^*_{X3C4}$ |
| O | 7.65 | 0.49 | 1.39 | 0.92 |
| S | 4.26 | 5.34 | 1.48 | 2.64 |
| Se | 3.01 | 8.51 | 1.18 | 3.04 |
| Te | 2.22 | 12.25 | 0.50 | 2.84 |

[a]Calculated at the HF/6-31G(d) level using Huzinaga basis for Se and Te with diffuse functions for d-orbitals.

Besides, the Cieplak modes predominate over the Felkin-Anh modes in all cases. It is strongly suggested that hyperconjugative stabilization involving the carbonyl $\pi$ orbital may be responsible for ground state conformational changes.

In conclusion, it is demonstrated again that the ground state conformational difference among these heterocyclic systems, affecting both the PDAS and EFOE density values, should be the origin of $\pi$-facial diastereoselection in six-membered ketones in general.

## *EXPERIMENTAL*

### *General Procedure for the Reduction of 2-Phenyl-1,3-diselenan-5-one (***3a***)*

To a solution of **3a** (0.05 mmol) in dry $Et_2O$ (4 mL) was added $LiAlH_4$ (0.1 mmol) under an $N_2$ atmosphere at 0°C. Then, the whole mixture was stirred at room temperature for ca. 2 hours. The reaction mixture was worked up by addition of saturated aqueous $NH_4Cl$ solution (4 mL), followed by extraction with $Et_2O$. Removal of the solvent under reduced pressure gave the crude product as a white solid. Purification of the residue by chromatography (hexane:EtOAc = 30:1) afforded the product as a colorless crystal. Satisfactory analytical and spectral data were obtained for all new compounds. Selected data for some compounds are as follows.

### *2-Phenyl-1,3-diselenan-5-one (3a)*

White solid, m.p. 101–103°C. IR (KBr): 3448, 2924, 2854, 1700, 1448, 1114, 698 cm$^{-1}$; $^1$H NMR (500 MHz, $CDCl_3$) $\delta$: 3.41 (d, $J$ = 12, 2H), 3.92 (d, $J$ = 12, 2H), 6.04 (s, 1H), 7.22–7.37 (m, 3H), 7.50–7.60 (m, 2H); $^{13}$C NMR (125 MHz, $CDCl_3$) $\delta$: 29.5, 30.2, 127.6, 128.7, 129.0, 138.2, 204.6; Ms *m/z*: 308 ($M^+$, $^{80}$Se, $^{80}$Se), 306 ($M^+$, $^{80}$Se, $^{78}$Se), 304 ($M^+$, $^{78}$Se, $^{78}$Se), 249, 247, 245, 170, 168, 167, 166, 103.

### *cis-2-Phenyl-1,3-diselenan-5-ol (6b)*

White solid, m.p. 131–132.5°C; IR (KBr): 3483, 2919, 1421, 1389, 1035, 697 cm$^{-1}$; $^1$H NMR (500 MHz, $CDCl_3$) $\delta$: 2.96 (dd, $J$ = 4.5, 13, 2H), 3.42 (dd, $J$ = 1, 13, 1H), 3.53 (d, $J$ = 12, 1H), 3.60–3.63 (m, 1H), 5,23 (s, 1H), 7.19–7.38 (m, 4H), 7.44–7.48 (m, 1H); $^{13}$C NMR (125 MHz, $CDCl_3$) $\delta$: 28.9, 34.5, 54.5, 127.5, 128.3, 128.9; Ms *m/z*: 306 ($M^+$, $^{80}$Se, $^{80}$Se), 304 ($M^+$, $^{80}$Se, $^{78}$Se), 304 ($M^+$, $^{78}$Se, $^{78}$Se), 249, 247, 245, 170, 168, 167, 166, 146, 103. Recrystallization of the **6b** from hexane and $CH_2Cl_2$ gave crystal which was suitable for X-ray analysis. Crystallographic data for **6b**: A Rigaku AFC6S diffractometer was employed with the Mo K$\alpha$ ($\lambda$ = 0.71073 Å) radiation monochromatized by graphite. Intensity data were collected using an $\omega$-2$\theta$ scan technique to a maximum 2$\theta$ value of 55.0°. A total of 4870 reflections were collected. The structure was solved by the direct method (SIR-92) [25]. The final full-matrix least-squares refinement of $F^2$ against all unique 2438 reflections ($R_{int}$ = 0.039) was performed by using the SHELXL-97 program [26]. The crystal data obtained are as follows:

Formula, $C_{10}H_{12}OSe_2$; $M$, 306.12; Space group, monoclinic $P21/c$; $a$, 12.460(2) Å; $b$, 5.657(3) Å; $c$, 15.233(2) Å; $\beta$, 96.659(13)°; $V$, 1066.5(6) Å$^3$; $Z$, 4; $\mu$, 6.892 mm$^{-1}$; $D_c$, 1.907 g/mL; $T$, 296 K; Size, 0.40 × 0.30 × 0.20 mm; Number of variables, 166; $R(F^2)$, 0.069; $wR(F^2)$, 0.079. The graphical molecular structure of **6b** (Figure 1) was drawn using the ORTEP-3 program for Windows [27]. Complete lists of atomic coordinates, thermal parameters, and bond parameters have been deposited at the Cambridge Crystallographic Data Centre (No. CCDC-155117).

## *APPENDIX: THEORETICAL DESCRIPTION OF THE EFOE MODEL*

As noted earlier, the simplest answer to the origin of π-facial stereoselectivity would be the π-facial difference in rate constants. The Salem–Klopman equation (Equation 1) [6], a simple kinetic equation, which expresses the driving force of a chemical reaction by the summation of three independent terms, was thought to provide a reasonable basis to construct a new theory of π-facial selection.

$$\Delta E = \underbrace{-\sum_{ab}(q_a + q_b)\beta_{ab}S_{ab}}_{\text{1st term}} + \underbrace{\sum_{k<l}\frac{Q_kQ_l}{r_{kl}}}_{\text{2nd term}} + \underbrace{\sum_{s}^{\text{occ.}}\sum_{r}^{\text{unocc.}} - \sum_{s}^{\text{occ.}}\sum_{r}^{\text{unocc.}} \frac{2\left(\sum_{ab} c_{ra}c_{sb}\beta_{ab}\right)^2}{E_r - E_s}}_{\text{3rd term}} \quad \text{(A1)}$$

where $q_a$, $q_b$ = electron populations in atomic orbital a or b; $\beta$ = resonance integral; $S$ = overlap integral; $Q_k$, $Q_l$ = total electron densities at atom $k$ or $l$; $r_{kl}$ = distance between atoms k and l; $E_r$ = energy level of $MO_r$; and $c$ = molecular orbital coefficients.

The first term of Equation A1 is the exchange repulsion term, which corresponds to the interactions among filled orbitals of the reactants. This term always leads to the destabilization of the system and is generally considered as steric effect in organic chemistry. The second term is the electrostatic interaction term that is especially important in ionic reactions. The third term is the donor–acceptor orbital interaction term, which should always lead to stabilization of the reacting system and to which the frontier orbital interaction between reactants generally contributes most. Among these three terms, Salem and Klopman pointed out that the first and the third terms should be particularly important in common organic reactions [6].

The EFOE model also focuses on the first and third terms of this equation. It is designed for quantitative evaluation of these two terms to identify essential factors of π-facial stereoselectivity of addition reactions of π-systems in general including ketones, alkenes, and enolates, etc., and eventually to predict π-facial stereoselectivity with some simple calculations and rules. Two new quantities π-plane-divided accessible space (PDAS) as the steric effect term and the exterior frontier orbital electron density (EFOE density) as the orbital interaction term—constitute the new model. Both quantities focus on the exterior area of a molecule.

## *π-PLANE-DIVIDED ACCESSIBLE SPACE (PDAS)*

Steric effect is commonly introduced only as a qualitative term in organic chemistry. Highly practical asymmetric syntheses have been designed through intuitive estimation of steric effects based on the size of substituents, such as A-values [23,28] or the van der Waals radius [29]. However, it is often difficult to predict steric effects of π-facial selection intuitively, in particular, for substrates having complex substituents around a π-bond. A simple quantity of π-facial steric effect should provide convenient means to gain clearer and more effective perception in designing organic synthesis. Described herein is the first method of π-facial steric effect calculation that is useful for common organic unsaturated substrates.

The new method focuses on three-dimensional space outside the van der Waals surface of a reactant molecule [30]. It is based on the simple assumption that the volume of the outer (exterior) space nearest to a reaction center should contain steric information of the reactant (substrate), since this volume is precisely the three-dimensional space available for

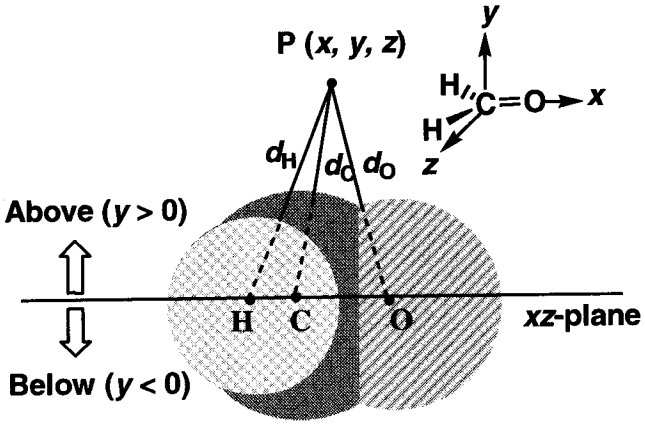


**FIGURE A1** Definition of π-plane-divided accessible space (PDAS) for the case of formaldehyde.

the reagent to access the reaction center of the substrate. The exterior volume is calculated for two faces of $\pi$-plane separately. Figure 5 illustrates the definition of $\pi$-plane-divided accessible space (PDAS) as a reasonable quantitative measure of $\pi$-facial steric effect using formaldehyde as an example. Molecular surface is defined as an assembly of spherical atoms having the van der Waals radii [29]. Integration of exterior three-dimensional space for the PDAS of the carbonyl carbon is performed according to the following conditions. If a three-dimensional point P($x,y,z$) outside the repulsive surface is the nearest to the surface of the carbonyl carbon (a reaction center on $xy$ plane) (i.e., if the distance between P and the van der Waals surface of the carbonyl carbon ($d_C$) is the shortest compared with the distance from P to other atomic surface (two $d_H$ and one $d_O$) and if the point is located above the carbonyl plane ($y > 0$), the space at this point is assigned to the above space of the carbonyl carbon.

The integration (summation) of such points is defined as the PDAS of the carbonyl carbon for the above plane. For the sake of convenience, spatial integration is limited to 5 au (2.65 Å) from molecular surface, where extension of an electronic wave function is negligible beyond this limit. In general, the carbonyl plane is defined as the plane that includes the two $sp^2$ atoms of the $\pi$-bond and is parallel with the vector connecting the two atoms at the $\alpha$-positions. The basic concept of PDAS definition is readily extended to other $\pi$-facial steric effect in compounds containing a general double bond other than carbonyl.

## *EXTERIOR FRONTIER ORBITAL EXTENSION DENSITY*

The importance of the exterior area of a substrate on $\pi$-facial stereoselection has also been quantified by the definition of exterior frontier orbital extension density (EFOE density), which represents the third term of Equation A1. Thus the $\pi$-plane-divided EFOE density (EFOE density) is defined as the integrated (summed) electron density of frontier orbital (HOMO for electrophilic addition ore LUMO for nucleophilic addition) [24] over specific exterior points over one face of the $\pi$-plane of a substrate molecule satisfying the following condition: the absolute total value of the wave functions belonging to the carbonyl carbon makes a maximum contribution to the total value of FMO wave function at the point. Such a condition guarantees that the driving force vector on hydride or other reagent is maximally directed toward the $sp^2$ reaction center. Thus integration of FMO probability density ($\Psi^2_{FMO}$) over such three-dimensional subspace ($\Omega$) that satisfies the previous condition should afford a reasonable quantitative measure of the third term of Equation 1. The values of EFOE density are expressed in percent for the sake of numerical convenience by normalizing the wave function ($\Psi_{FMO}$) to 100 (Equation A2).

$$\text{EFOE density } (\%) = 100 \times \int \Psi^2_{FMO}\, d\Omega \quad \text{(A2)}$$

## *ACKNOWLEDGMENT*

It is a great pleasure for the authors to join the special occasion of 72nd birthday celebration of Professor N. Inamoto by contributing their recent theoretical work on heterocyclic compounds, a part of which has been summarized by S.T. in a recent review article [4]. Professor Inamoto's ingenious work in organic chemistry has always been a stimulus guide to S.T. since his graduate days.

## *REFERENCES*

[1] Gung, B. W.; le Noble, W. J., Eds. Chem Rev (special issue on Diastereoselection) 1999, 99, 1067.
[2] (a) Cherest, M.; Felkin, H. Tetrahedron Lett 1968, 2205; (b) Cherest, M.; Felkin, H.; Prudent, N. Tetrahedron Lett 1968, 2199; (c) Anh, N. T.; Einsenstein, O.; Lefour, J. M-.; Tran Huu Dau, M. E. J Am Chem Soc 1976, 95, 6146; (d) Anh, N. T.; Einsenstein, O. Nouv J Chim 1976, 1, 61.
[3] Cieplak, A. S. J Am Chem Soc 1981, 103, 4540.
[4] Tomoda, S. Chem Rev 1999, 99, 1243.
[5] (a) Tomoda, S.; Senju, T. Tetrahedron 1997, 53, 9057; (b) Tomoda, S.; Senju, T. Chem Comm 1999, 621.
[6] (a) Klopman, G. J Am Chem Soc 1968, 90, 223; (b) Salem, L. J Am Chem Soc 1968, 90, 543; (c) Fleming, I. Frontier Orbitals and Organic Chemical Reactions; Wiley & Sons: London, 1977.
[7] (a) Tomoda, S.; Senju, T. Tetrahedron 1999, 55, 3871; (b) S. Tomoda, S.; Senju, T. Tetrahedron 1999, 55, 5303; (c) Tomoda, S.; Senju, T. Chem Lett 1999, 625; (d) S. Tomoda, S.; Senju, T. Chem Lett 1999, 353; (e) Tomoda, S.; Senju, T.; Kawamura, M.; Ikeda, T. J Org Chem 1999, 64, 5396.
[8] Tomoda, S.; Kaneno, D.; Senju, T. Chem Lett 1999, 1115.
[9] Jochims, J. C.; Kobayashi, Y. M.; Skrzelewski, E. Tetrahedron Lett 1974, 571, 575.
[10] Kobayashi, Y. M.; Lambrecht, J.; Jochims, J. C.; Burkert, U. Chem Ber 1978, 111, 3442.
[11] Wu, Y. D.; Houk, K. N. J Am Chem Soc 1987, 109, 908.
[12] (a) Wu, Y. D.; Houk, K. N.; Paddon-Row, M. N. Angew Chem 1992, 104, 1087; (b) Angew Chem Int Ed Engl 1992, 31, 1019; (c) Wu, Y. D.; Houk, K. N. J Am Chem Soc 1993, 115, 10992.
[13] Tomoda, S.; Senju, T. Chem Comm 1999, 423.
[14] (a) Frisch, M. J.; Trucks, G. W.; Schlegel, H. B.; Gill,

P. M. W.; Johnson, B. G.; Robb, M. A.; Cheeseman, J. R.; Keith, T.; Petersson, G. A.; Montgomery, J. A.; Raghavachari, K.; Al-Laham, M. A.; Zakrzewski, V. G.; Ortiz, J. V.; Foresman, J. B.; Cioslowski, J.; Stefanov, B. B.; Nanayakkara, A.; Challacombe, M.; Peng, C. Y.; Ayala, P. Y.; Chen, W.; Wong, M. W.; Andres, J. L.; Replogle, E. S.; Gomperts, R.; Martin, R. L.; Fox, D. J.; Binkley, J. S.; Defrees, D. J.; Baker, J.; Stewart, J. P.; Head-Gordon, M.; Gonzalez, C.; Pople, J. A.; GAUSSIAN94, revision D.1 and E.2; Gaussian, Inc.: Pittsburgh, 1995; (b) Frisch, M. J.; Trucks, G. W.; Schlegel, H. B.; Scuseria, G. E.; Robb, M. A.; Zakrzewski, V. G.; Montgomery, J. A., Jr.; Stratmann, R. E.; Burant, J. C.; Dapprich, S.; Millam, J. M.; Daniels, A. D.; Kudin, K. N.; Strain, M. C.; Farkas, O.; Tomasi, J.; Barone, V.; Cossi, M.; Cammi, R.; Mennucci, B.; Pomelli, C.; Adamo, C.; Clifford, S.; Ochterski, J.; Petersson, G. A.; Ayala, P. Y.; Cui, Q.; Morokuma, K.; Malick, D. K.; Rabuck, A. D.; Raghavachari, K.; Foresman, J. B.; Cioslowski, J.; Ortiz, J. V.; Stefanov, B. B.; Liu, G.; Liashenko, A.; Piskorz, P.; Komaromi, I.; Gomperts, R.; Martin, R. L.; Fox, D. J.; Keith, T.; Al-Laham, M. A.; Peng, C. Y.; Nanayakkara, A.; Gonzalez, C.; Challacombe, M.; Gill, P. M. W.; Johnson, B.; Chen, W.; Wong, M. W.; Andres, J. L.; Gonzalez, C.; Head-Gordon, M.; Replogle, E. S.; Pople, J. A. GAUSSIAN98 revision A.5; Gaussian, Inc.: Pittsburgh, 1998.

[15] (a) Becke, A. D. Phys Rev A 1988, 38, 3098; (b) Becke, A. D. J Chem Phys 1993, 98, 5648; (c) Lee, C.; Yang, W.; Parr, R. G. Phys Rev B 1988, 37, 785.

[16] Perdew, J. P.; Wang, Y. Phys Rev B 1992, 45, 13244.

[17] Huzinaga, S. Gaussian Basis Sets for Molecular Calculations; Elsevier: Amsterdam, 1984.

[18] Reed, A. E.; Curtiss, L. A.; Weinhold, F. Chem Rev 1988, 88, 899 (NBO program version 4.0 was used throughout this work).

[19] The UNIX FORTRAN 77 codes are available upon request by e-mail: tomoda@selen.c.u-tokyo.ac.jp

[20] (a) Krief, A.; Defrere, L. Tetrahedron Lett 1996, 37, 2667; (b) Clarembeau, M.; Cravador, A.; Dumont, W.; Hevesi, L.; Krief, A.; Lucchietti, J.; van Ende, D. Tetrahedron 1985, 41, 4793; (c) Baucom, K. B.; Butler, G. B.; J Org Chem 1972, 37, 1730; (d) Albert, G.; Butler, B.; J Org Chem 1977, 42, 676; (e) Klayman, D. L.; Griffin, T. S.; J Am Chem Soc 1973, 95, 197; (f) Syper, I.; Mlochwski, J.; Synthesis 1984, 439. Detailed procedure for the synthesis of **3a** will be reported elsewhere.

[21] Tomoda, S.; Kaneno, D.; Senju, T. Heterocycles 2000, 52, 1435.

[22] Percent bond elongation (%BE) = $(\Delta r/r_S) \times 100$, where $\Delta r$ = the difference in the bond lengths between the vicinal antiperiplanar (AP) bond in transition state ($r_{TS}$) and the corresponding bond of starting ketone ($r_S$); $\Delta r = r_{TS} - r_S$.

[23] Eliel, E. L.; Wilen, S. H.; Mander, L. N. Stereochemistry of Organic Compounds; Wiley & Sons: New York, 1994; p 695.

[24] (a) Fukui, K. Theory of Orientation and Stereoselection; Springer Verlag: Heidelberg, 1979; (b) Fukui, K.; Fujimoto, H. Frontier Orbitals and Reaction Paths; World Scientific: London, 1997.

[25] Altomare, A.; Cascarano, G.; Giacovazzo, C.; Guagliardi, A.; Burla, M. C.; Polidori, G.; Camalli, M. J Appl Crystallogr 1994, 27, 435–436.

[26] Sheldrick, G. M. SHELXL97: Program for the Refinement of Crystal Structures; University of Göttingen: Göttingen, Germany, 1997.

[27] Farrugia, L. J. ORTEP-3 for Windows, version 1.03; University of Glasgow: Glasgow, Scotland, 1997.

[28] Wistein, S.; Holness, N. J. J Am Chem Soc 1955, 89, 5562.

[29] Bondi, A. J Phys Chem 1964, 68, 441.

[30] Ohno, S.; Matsumoto, S.; Harada, Y. J Chem Phys 1984, 81, 4447.